RIELAC
Revista de Ingeniería Electrónica,
Automática y Comunicaciones

Modeling and Event-Driven Simulation of a Photovoltaic System Controlled with Two Configurations of Perturb & Observe Maximum Power Point Tracking

Guillermo Gallo, Juan Ruiz, Mario Bolaños, Gustavo Osorio, Fabiola Angulo

ABSTRACT/*RESUMEN*

In this article, a photovoltaic system is modeled and simulated in order to compare two different approaches of maximum power point tracking control structures. First, the system uses a Perturb & Observe maximum power point tracking control directly applied to the duty cycle, and its simulations results are compared with the experimental ones obtaining a good agreement. Then, an average current-mode control structure is coupled to the maximum power point tracking controller and simulations are performed for both systems. The system that incorporates current-mode control exhibits better response when perturbations are present, improving the settling time and reducing the steady-state oscillations.

Keywords: Solar Energy, Piecewise Linear Analysis, Average Current Control Mode, DC/DC Power Converters, Maximum Power Point Tracking.

En este artículo se modela y simula un sistema fotovoltaico con el objeto de comparar dos estructuras de control para el seguimiento del punto de máxima potencia, lo cual se hace en dos partes. En la primera parte, el sistema se controla con el algoritmo de seguimiento del punto de máxima potencia llamado Perturbe & Observe, el cual se aplica directamente al ciclo útil. Así mismo, se obtienen resultados de simulación que se comparan con los resultados experimentales presentándose una alta concordancia. En la segunda parte, al algoritmo de seguimiento del punto de máxima potencia se le acopla una estructura de control en modo de corriente promediada, y se comparan a través de simulaciones la robustez de ambos sistemas ante perturbaciones. El sistema que incluye el control en modo de corriente presenta una mejor respuesta tanto en el tiempo de establecimiento como en las oscilaciones de estado permanente.

Palabras Claves: Energía solar, análisis lineal suave a trozos, control en modo de corriente promediada, convertidores de potencia DC/DC, seguimiento del punto de máxima potencia.

Modelado y simulación orientada a eventos de un sistema fotovoltaico controlado con dos configuraciones de seguimiento del punto de máxima potencia con Perturbe & Observe.

1.-INTRODUCTION

Photovoltaic (PV) energy is a locally available renewable resource with a lower carbon footprint which becomes essential to counteract the environmental impacts caused by the growing use of the conventional fossil fuels. In addition, recent efforts seek to make the use of this kind of energy more feasible improving the efficiency of the system and formulating governmental policies to encourage its use. For instance, the solar PV global capacity has increased from 16 GW in 2008 to 227 GW in 2015 [1], and its study has become more attractive to researches of different fields.

A PV system is mainly composed by the elements shown in Figure 1. The PV source transforms the sunlight into electricity, it has a nonlinear behavior with a Maximum Power Point (MPP) described by the current-voltage curve (I-V) and the power-voltage curve (P-V) [2-5]. The MPP is constantly changing according to the environmental conditions; hence it is necessary to adopt an intermediate stage between the PV source and the load, known as a Maximum Power Point Tracking (MPPT) system. MPPT guarantees the highest energy harvesting possible. The load may be represented by a resistance in the case of a non-regulated DC bus, or it can also be represented by a constant voltage load, in the case of a regulated DC bus or a battery, [6, 7].
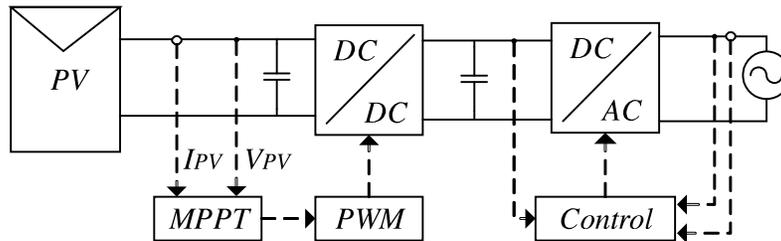

Figure 1
PV system control.

The MPPT system is composed mainly of a DC-DC converter [8], controlled by an MPPT algorithm [9-12] which is capable of matching the electrical characteristics of the connected load to the MPP characteristics located in the P-V curve. There are some works in the literature where the MPPT algorithm directly affects the duty cycle of the converter [13], presenting an inadequate voltage or current regulation such that the converter presents an increased switching stress and losses [14]. Other works in the literature present the MPPT systems accompanied by control structures that improve the performance of its steady and transient states [14, 15]. For instance, the presence of a proportional and integral controller can reduce losses and stress, and can improve the settling time of the converter and avoids oscillation and overshoot [16, 17].

In this work, a PV System was modeled and simulated in order to compare two different approaches of MPPT control structures (Figure 2). First, the system was controlled with Perturb & Observe MPPT which is directly applied to the duty cycle and the simulations results were performed and compared with the experimental results. Then, an average current-mode control structure was coupled to the MPPT, improving the settling time and reducing the steady-state oscillations. For these tests, an event driven simulation based on hybrid systems that includes the complete PV source dynamics is proposed. The hybrid systems combine the structures of differential equation systems with discrete maps [18]. This kind of approach may present sliding dynamics that introduces simulation issues [19, 20]. In order to solve this problem, the equations that describe the sliding zones are found and considered in the modeling.
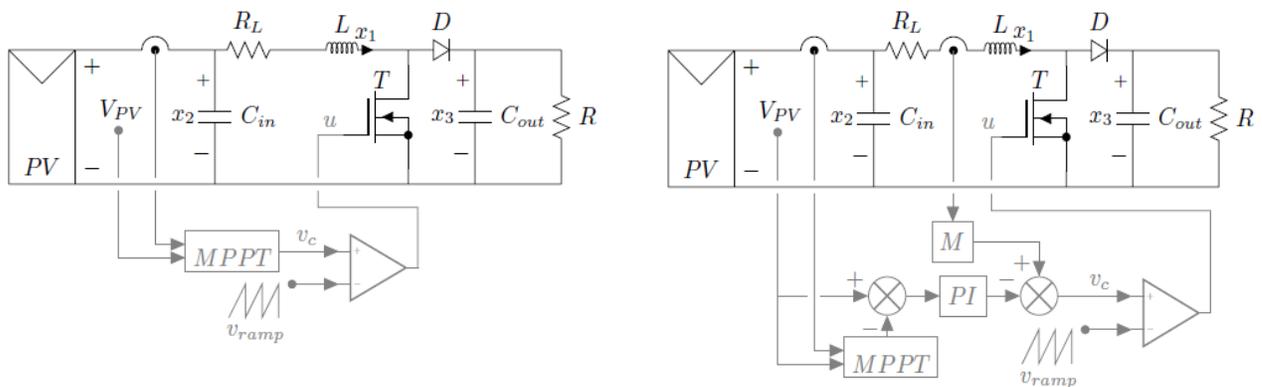

Figure 2
PV system with two MPPT control configurations: a) P&O, b) P&O coupled with an average current-mode control.

This paper is organized as follows. In section 2, a brief description of Perturb & Observe MPPT, the modeling and identification of the panel, and the hybrid model of the whole system for each control configuration are presented. In section 3, the numerical and experimental results and the comparison between the two control configurations are studied. In section 4, the corresponding conclusions and future work are discussed.

2.-PERTURB & OBSERVE MAXIMUM POWER POINT TRACKING

Solar panels are formed by arrays of solar cells, which convert radiation from the sun into useful electricity. Each cell has only one MPP, and it depends on external factors such as temperature and radiation. The MPPT is done by varying the operating point of the panel in such a way that the solar system can deliver the maximum possible power. One way to change the operating point of the panel is by varying the load that is connected to its terminals. Load variations are controlled by a DC-DC power converter, which has the characteristic of increasing or reducing the resistance sustained at the panel terminals, by modifying the duty cycle.

To track the MPP means a breakthrough in improving the efficiency of photovoltaic systems. Although several methods exist in the literature, one of the most widely used algorithms is the Perturb and Observe (P & O), thanks to its performance and simplicity. This algorithm is based on perturbing a control parameter by small steps and observing the changes of the power, forcing the system to iterate around the MPP.

The fundamental principle of the control strategy is to obtain the digital PWM signal through continuous iteration of the duty cycle around an operation point. The algorithm starts by taking note of voltage V_{PV} and current I_{PV} at the terminals of the PV panel in order to calculate the power delivered by the source. After perturbing the duty cycle, it is necessary to measure the power again. If the system power increases, the MPPT algorithm perturbs the duty cycle in the same direction, otherwise, the perturbation is in the opposite direction.

The systems considered in this work are shown in Figure 2. They consist of two photovoltaic MPPT systems based on a boost converter structure that feeds a resistive load. The PV system exhibits a high nonlinear complexity due to the characteristics of the PV source and the nonlinear elements such as the semiconductors in the DC-DC converter. Therefore, its modeling and simulation may result in a challenging problem. For instance, different approaches have been proposed in the literature such as the linearization of the PV system and the simplification of the PV module in a constant voltage or a constant current source, [14, 21-23]. However, in order to have a deeper understanding of the system, a modeling approach that includes not only the complete dynamics of the PV source, but also the high frequency components of the DC-DC converter should be taken into account.

2.1.-POTOVOLTAIC SOURCE MODELING

A photovoltaic panel can be mathematically modeled by theoretical equations based on an equivalent circuit, leading to different models that vary in complexity and precision. In order to describe the electrical behavior of the PV source, the five parameters model of Figure 3 is used. This model is the most widely used in the literature [24, 25], where a current source is used to model the incident radiation, the diode models the polarization phenomenon and the resistances R_S and R_P represent the power losses by connections in series and in parallel.
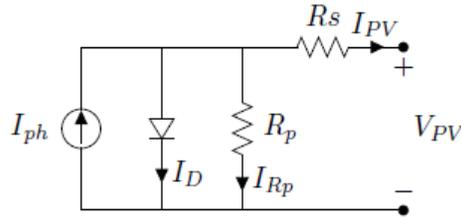

Figure 3

Five parameters model.

The mathematical equation that describes the model of the 5 parameters is given by the equation 1:

$$I_{PV} = I_{ph} - I_s \left(e^{\frac{V_{PV} + I_{PV} R_S}{N_s a V_T}} - 1 \right) - \frac{V_{PV} - I_{PV} R_S}{R_P} \qquad (1)$$

where:

I_{PV}:   Current at the terminals of the panel.
I_{ph}:   Photo-generated current.
V_{PV}:   Voltage at the terminals of the panel.
R_S: Equivalent series resistance.
R_P: Equivalent parallel resistance.
I_s: Saturation current of the diode.

a:	Diode ideality factor.
N_s:	Number of cells connected in series.
V_T:	Thermal diode voltage.

The equation 1 is an implicit one and it is usually solved using numerical methods, such as Newton Raphson. However, from a simulation point of view, this approach may lead to longer simulation times and convergence problems. Therefore, it is necessary to express the equation 1 in an explicit way, using the Lambert W approach [26].

On the other hand, the PV arrays do not exhibit a linear relationship *V-I*, and parameters such as parasitic resistances R_P and R_S need to be adjusted with experimental data or with special devices because most commercial panels do not provide this information. In [24] the parameters of R_P and R_S are calculated from an iterative process that adjusts the *V-I* curve with the basic data provided by the manufacturer, such as short circuit current, open circuit voltage, current and voltage at the MPP and maximum power. In this way, it is possible to estimate the parameters for a reliable model of the solar panel without resorting to specialized measuring devices. We used the solar panel *SYK50-18M*. Table 1 shows its characteristic data at standard test conditions; temperature of *25°C* and radiation of *1000 W/m²*.

Behavior under standard conditions	STD
Power at the MPP (P_{max})	*50W*
Open circuit voltage (V_{oc})	*22.24V*
Voltage at MPP (V_{mpp})	*18V*
Short circuit current (I_{sc})	*3.06A*
Current at MPP (I_{mpp})	*2.78A*
TC I_{sc}	*0.034 % / °K*
TC U_c	*-0.34 % / °K*
Cell number N_s	*36*
Diode ideality factor a	*1.3*
Parallel resistance R_P	*454.9310 Ω*
Series resistance R_S	*0.2660 Ω*

Table 1
Parameters for a solar panel SYK50-18M.

The graphs in Figure 4 were simulated with parameters R_P and R_S obtained as is shown in [24]. In Figure 4(a) and 4(b) show the *V-I* and *V-P* curves, respectively, for a variant radiation. Figures 4(c) and 4(d) show the behavior of the source under temperature variations.
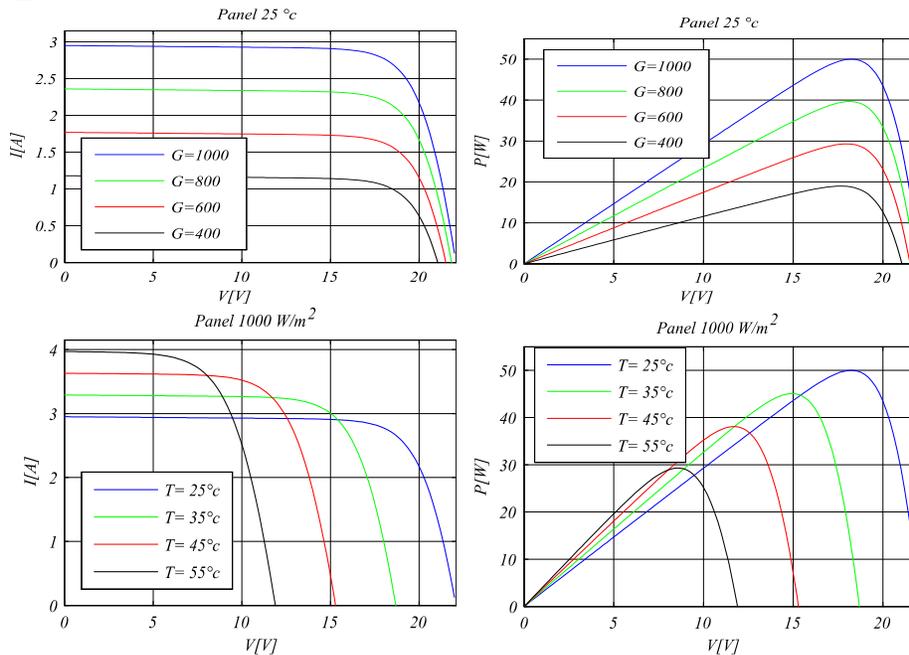

Figure 4
Voltage vs. current and voltage vs. power delivered by a PV panel. Variation in (a), (b) radiation and (c), (d) temperature.

2.2.-HYBRID SYSTEM MODELING

Both systems of Figure 2 present three configurations or states depending on the values (*ON*, *OFF*) of the diode and the transistor (Table 2).

State	T	D
s_1	ON	OFF
s_2	OFF	ON
s_3	OFF	OFF

Table 2

State transition table.

Figure 5 depicts the three circuit configurations of both solar systems.
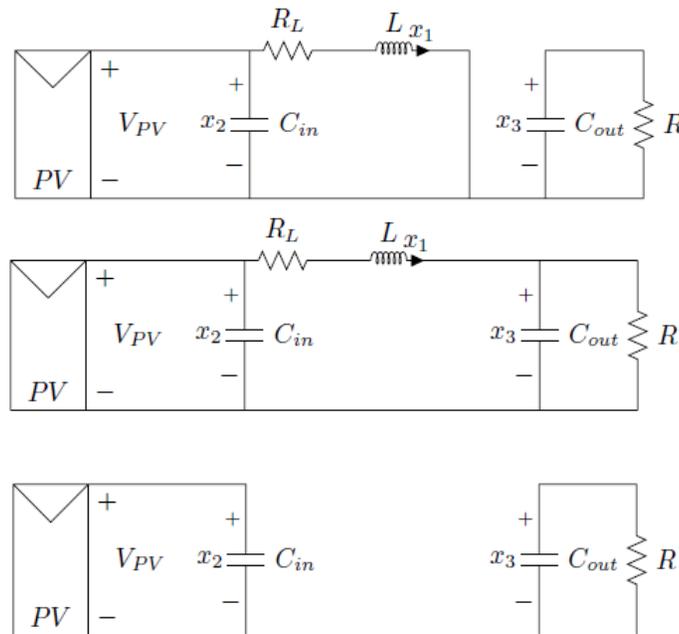
Figure 5

Circuit configurations: a) State 1: *T=ON, D=OFF*, b) State 2: *T=OFF, D=ON*, c) State 3: *T=OFF, D=OFF*.

The whole system can be expressed as:

$$\dot{x} = A_i x + B \qquad (2)$$

where $x: = [x_1\ x_2\ x_3]^{\mathrm{T}}$ and $i \in \{1,2,3\}$. x_1 is the inductor current, x_2 is the voltage at the terminal of C_{in} and x_3 is the voltage at the terminals of C_{out}. The matrices A and B are different for each control structure.

2.2.1.-FIRST CONTROL STRUCTURE

This system is third order and its matrices A_i and B are defined as follows:

$$A_1 = \begin{bmatrix} -\dfrac{R_L}{L} & \dfrac{1}{L} & 0 \\ -\dfrac{1}{C_{in}} & 0 & 0 \\ 0 & 0 & -\dfrac{1}{RC_{out}} \end{bmatrix} ; A_2 = \begin{bmatrix} -\dfrac{R_L}{L} & \dfrac{1}{L} & -\dfrac{1}{L} \\ -\dfrac{1}{C_{in}} & 0 & 0 \\ \dfrac{1}{C_{out}} & 0 & -\dfrac{1}{RC_{out}} \end{bmatrix} ; A_3 = \begin{bmatrix} 0 & 0 & 0 \\ 0 & 0 & 0 \\ 0 & 0 & -\dfrac{1}{RC_{out}} \end{bmatrix} \tag{3}$$

$$B = \begin{bmatrix} 0 \\ \dfrac{f(x_2)}{C_{in}} \\ 0 \end{bmatrix} \tag{4}$$

where $f(x_2)$ is the explicit solution of the equation 1 using the Lambert W approximation, [26]. $f(x_2)$ gives the value of the panel current (I_{PV}) for an input voltage, x_2. The whole system may be represented by the hybrid automaton shown in Figure 6. In this automaton, the states s_i are associated to the matrices A_i and B. The conditions of transition are defined as: $c_{1,2}$: $u = 0$; $c_{2,1}$: $u = 1$; $c_{2,3}$: $x_1 = 0$; $c_{3,1}$: $u = 1$. The variable u is defined as follows:

$$u = \begin{cases} 1 & if \quad v_c \geq v_{ramp} \\ 0 & if \quad v_c < v_{ramp} \end{cases} \tag{5}$$

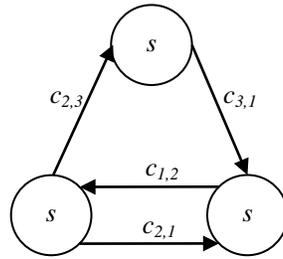v_c is the control signal with which the duty cycle is calculated.

Figure 6
Hybrid Automaton.

2.2.2.-SECOND CONTROL STRUCTURE

In this case, we add a new state variable x_4 corresponding to the integral of the error. A_i and B matrices are defined as follows:

$$A_1 = \begin{bmatrix} -\dfrac{R_L}{L} & \dfrac{1}{L} & 0 & 0 \\ -\dfrac{1}{C_{in}} & 0 & 0 & 0 \\ 0 & 0 & -\dfrac{1}{RC_{out}} & 0 \\ 0 & 1 & 0 & 0 \end{bmatrix} ; A_2 = \begin{bmatrix} -\dfrac{R_L}{L} & \dfrac{1}{L} & -\dfrac{1}{L} & 0 \\ -\dfrac{1}{C_{in}} & 0 & 0 & 0 \\ \dfrac{1}{C_{out}} & 0 & -\dfrac{1}{RC_{out}} & 0 \\ 0 & 1 & 0 & 0 \end{bmatrix} ; A_3 = \begin{bmatrix} 0 & 0 & 0 & 0 \\ 0 & 0 & 0 & 0 \\ 0 & 0 & -\dfrac{1}{RC_{out}} & 0 \\ 0 & 1 & 0 & 0 \end{bmatrix} \tag{6}$$

$$B = \begin{bmatrix} 0 \\ \dfrac{f(x_2)}{C_{in}} \\ 0 \\ -V_{ref} \end{bmatrix} \tag{7}$$

V_{ref} *is* calculated by the MPPT algorithm. This system can be represented by the hybrid automaton shown in Figure 6. The states s_i are associated to the matrices A_i and B. The conditions of transition are the same as the previous system. Furthermore, the variable u is defined by the equation 5. v_c is defined as:

$$v_c = k_p(x_2 - V_{ref}) + k_p k_i x_4 - M x_1 \qquad (8)$$

Where k_p, k_i and M are control constants. In this system, a sliding dynamic appears. This dynamic is defined by the states s_1 and s_2. The transition between these states is defined by the control variable v_c and the ramp signal v_{ramp}. When the control signal is over the ramp signal, the DC-DC converter works in the state 1 (s_1). In other case, the DC-DC converter works in the state 2 (s_2). There are some parameters values that force the v_c signal to slide on the ramp signal, which can block an event-driven simulation [18]. To overcome this drawback, a Filippov method is used to formulate a new field that flows onto the ramp, [19].

3.-NUMERICAL AND EXPERIMENTAL RESULTS

This section shows the simulation results and their comparison to the ones obtained experimentally for the first control structure. It also compares the system response to perturbations when both control structures are used.

Two main tests show the validity of the operation of the method P&O. The first is a sweep by varying the duty cycle of the PWM (*0% - 100%*), in order to observe what percentage of the cycle is at the MPP. The second test verifies that the algorithm finds the MPP and stays near to this point.

C_{in}	*100μF*
C_{out}	*220μF*
L	*20mH*
Sampling frecuency, F_s	*1kHz*
Perturbation Δ in P&O	*0.1*

Table 3

Desing parameters.

Simulations and experimental results were obtained using radiation *550W/m²*, load of *25Ω* and the parameters shown in Table 3. In Figure 7(a) and 7(b) a duty cycle sweep is performed from *0 % - 100 %*, the signal is represented by *Reference$_{PWM}$* which moves of *0-10*, being *10* the 100 % of *D*. A very good relationship between the simulated data and the data acquired experimentally is observed.
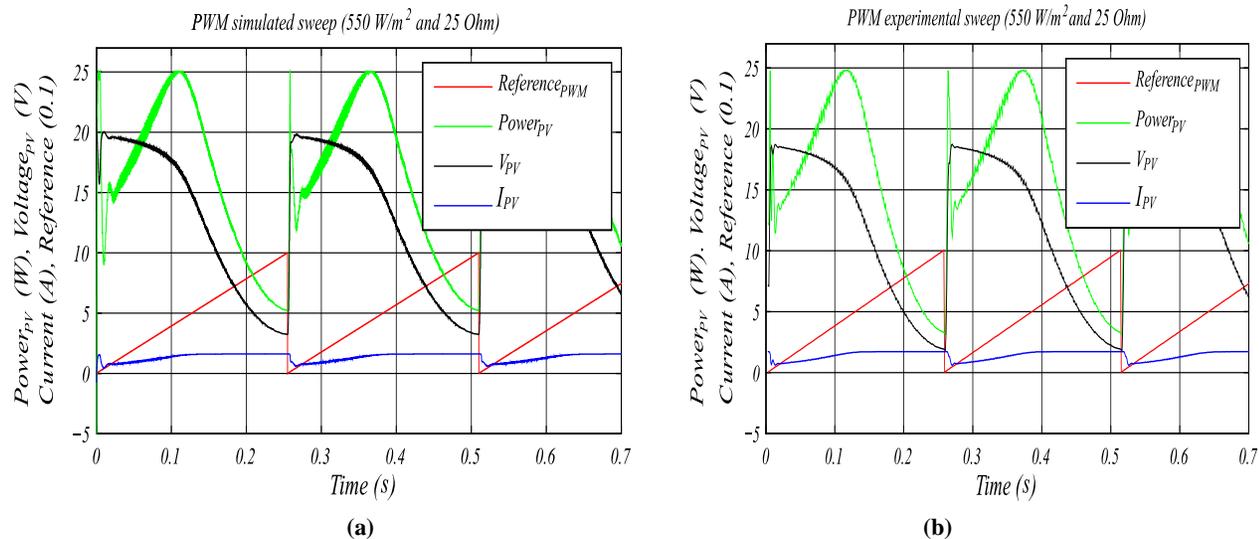

Figure 7

PWM sweep: a) simulated, b) experimental.

Figures 8(a) and 8(b) show how the MPPT algorithm achieves the MPP in simulation and also experimentally. The arrival times at MPP are very close and the differences lie in the impossibility to maintain constant radiation and temperature because the test took place under atmospheric conditions.
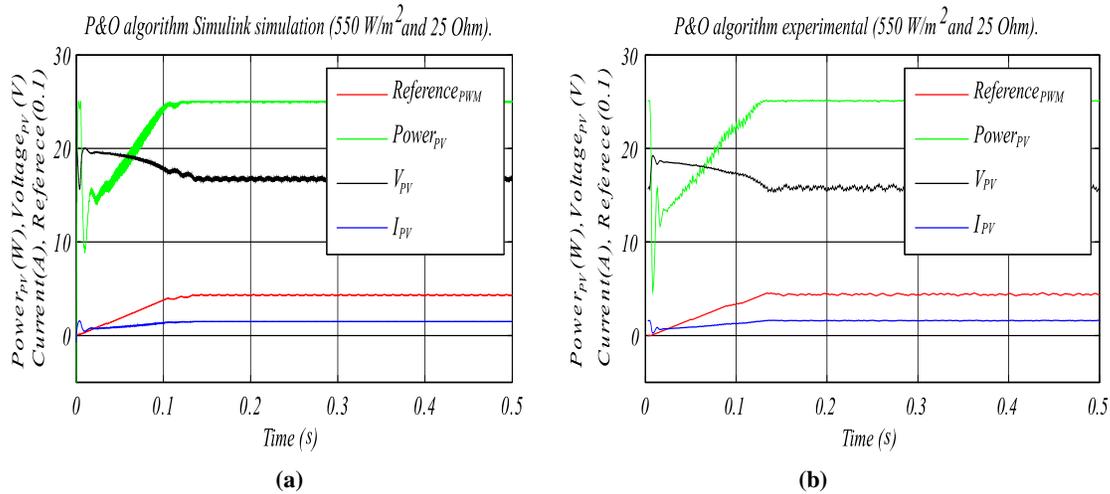

(a)   **(b)**

Figure 8

Perturb and observe algorithm: a) simulated, b) experimental.

Figure 9 shows a zoom of the duty cycle signal. The values vary periodically around the MPP, even though the graphics vary somewhat, there is concordance between the numerical and experimental results.
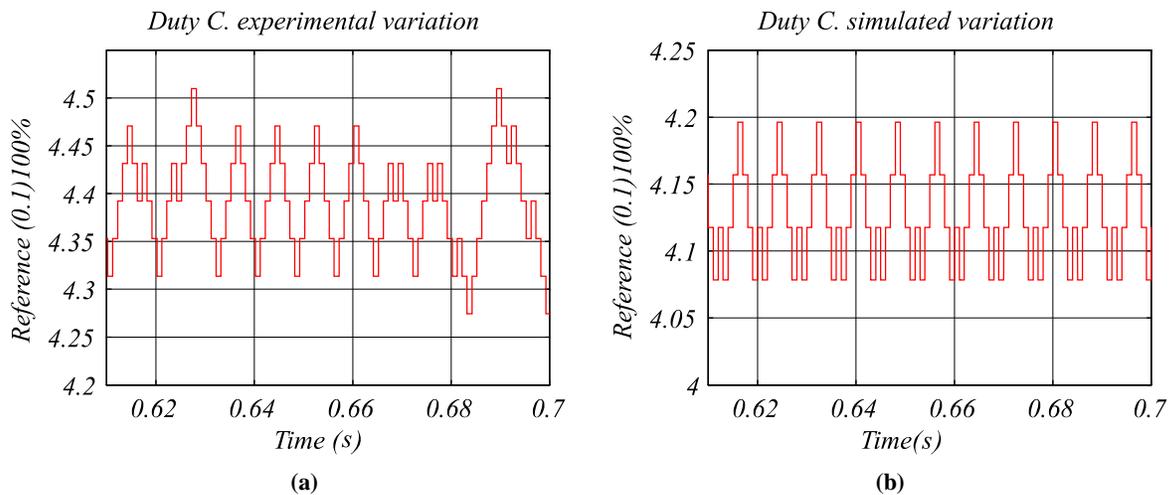

(a)   **(b)**

Figure 9

Zoom in PWM signal: a) experimental, b) simulated.

Tests with other radiation levels are also depicted, for example in Figure 10 a MPPT for a radiation of *390W/m²* and a load of *50Ω* are shown.

To compare the response to perturbation in power reference of both control structures a set of simulations were performed, using the parameters of the Table 3. The parameters of the PI controller are: $k_p=0.5$, $k_i=100$, and $M=2$. Figure 11 shows the response to perturbations in the two control structures when the power reference changes from *50W* to 15*W* at time *0.2s* and from *15W* to *40W* at time *0.4s*. It can be seen that the second control structure presents better settling times and lower steady-state oscillations.
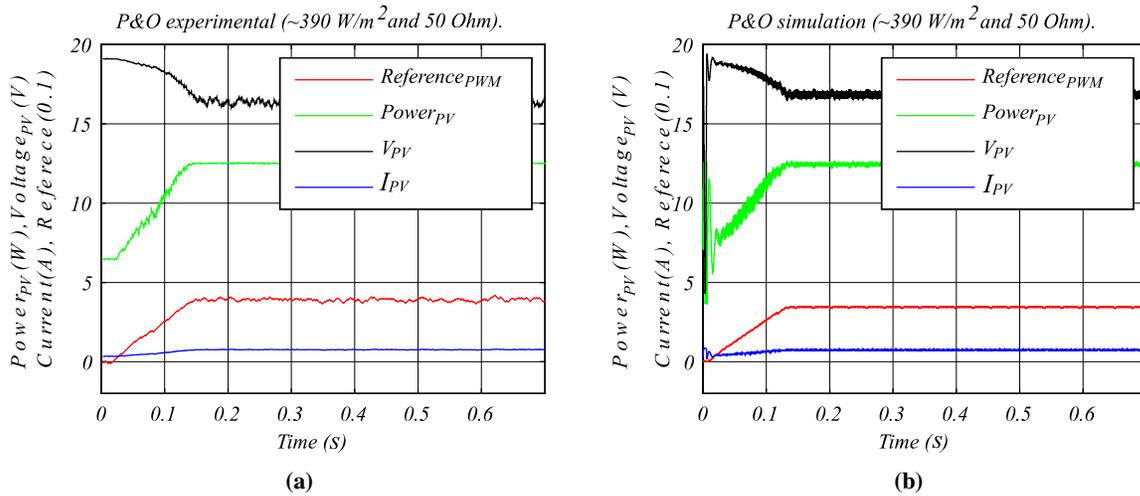
Figure 10

Results (a) experimental and (b) simulation for a radiation of *390W/m²* and *50*Ω.
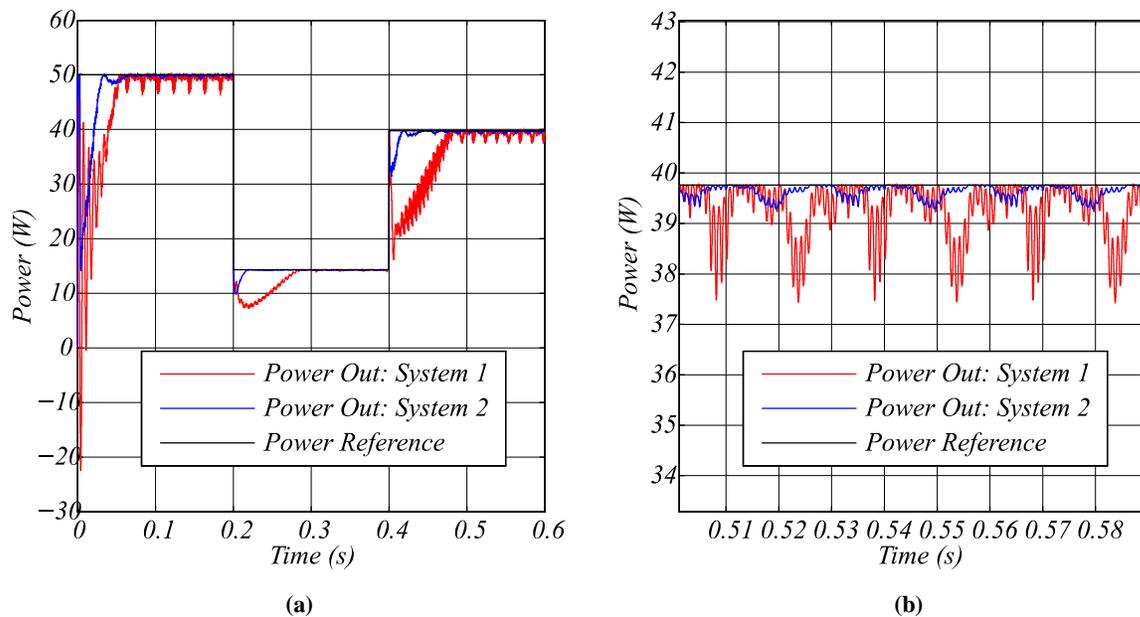

Figure 11

Comparison between the two control techniques: a) response to disturbances, b) zoom.

4.-CONCLUSIONS

In this work, simulation and experimental results of a photovoltaic system conformed by a solar source, a boost power converter, a Perturb and Observe algorithm and a purely resistive load are presented. The system was controlled with two MPPT structures. The first structure acts directly on the duty cycle of the converter. In the second structure, the MPPT control is coupled with an average current-mode control structure. The last structure improves the settling time and the steady-state oscillations of the converter; however, a sliding dynamic can appear. This kind of dynamics can rapidly deteriorate the semiconductors due to high switching frequencies. For this reason, it is necessary to tune the current-mode controller properly. Another alternative is to implement a peak current mode controller, which ensures a switching per ramp cycle.

Guillermo Gallo, Juan Ruiz, Mario Bolaños, Gustavo Osorio, Fabiola Angulo
RIELAC, Vol. XXXVIII 1/2017 p. 57-67 Enero - Abril ISSN: 1815-5928

ACKNOWLEDGEMENTS

REFERENCES

1. Ren PS. Renewables 2016 global status report. REN21 Secretariat: Paris, France. 2016.
2. Mahmoud Y, El-Saadany EF. A Photovoltaic Model With Reduced Computational Time. IEEE Trans Ind Electron. 2015;62(6):3534–44.
3. Chin VJ, Salam Z, Ishaque K. Cell modelling and model parameters estimation techniques for photovoltaic simulator application: A review. Vol. 154, Applied Energy. Elsevier Ltd; 2015. p. 500–19.
4. Tian H, Mancilla-David F, Ellis K, Muljadi E, Jenkins P. A cell-to-module-to-array detailed model for photovoltaic panels. Sol Energy. 2012;86(9):2695–706.
5. Barth N, Jovanovic R. Optimization and temperature dependence of the parameters of single and double diode electrical models for PV panels. Sol Energy Mater Sol Cells. 2016;513:87–98.
6. López J, Jr SIS, Donoso PF, Morais LMF, Cortizo PC, Severo MA. Digital control strategy for a buck converter operating as a battery charger for stand-alone photovoltaic systems q. Sol Energy. 2016;140:171–87.
7. Farahat MA, Metwally HMB, Mohamed AA. Optimal choice and design of different topologies of DC e DC converter used in PV systems , at different climatic conditions in Egypt. Renew Energy. 2012;43:393–402.
8. Rashid MH. Power Electronics Ciruits, Devices, and Applications. Fourth Edi. Pearson/Prentice Hall; 2014. 526-530 p.
9. Verma D, Nema S, Shandilya AM, Dash SK. Maximum power point tracking (MPPT) techniques: Recapitulation in solar photovoltaic systems. Renew Sustain Energy Rev. 2016;54:1018–34.
10. De Brito MAG, Galotto L, Sampaio LP, De Azevedo Melo G, Canesin CA. Evaluation of the main MPPT techniques for photovoltaic applications. IEEE Trans Ind Electron. 2013;60(3):1156–67.
11. Rezk H, Eltamaly AM. A comprehensive comparison of different MPPT techniques for photovoltaic systems. Sol Energy. 2015 Feb;112:1–11.
12. Liu L, Meng X, Liu C. A review of maximum power point tracking methods of PV power system at uniform and partial shading. Renew Sustain Energy Rev. 2016;53:1500–7.
13. Femia N. Power Electronics and Control Techniques For Maximum Energy Harvesting in Photovoltaic System. crc press; 2013.
14. Villalva MGG, de Siqueira TGG, Ruppert E. Voltage regulation of photovoltaic arrays: small-signal analysis and control design. IET Power Electron. 2010 Nov;3(6):869.
15. Mamarelis E, Petrone G, Spagnuolo G, Member S. Design of a Sliding-Mode-Controlled SEPIC for PV MPPT Applications. IEEE Trans Ind Electron. 2014;61(7):3387–98.
16. Villalva MG, Gazoli JR, Filho ER. Analysis and Simulation of the P&O Mppt Algorithm Using a Linearized Pv Array Model. 2009 Brazilian Power Electron Conf. 2009;189–95.
17. Venturini RP, Scarpa VVR, Spiazzi G, Buso S. Analysis of limit cycle oscillations in maximum power point tracking algorithms. In: 2008 IEEE Power Electronics Specialists Conference. 2008. p. 378–84.
18. Acary V, Bonnefon O, Brogliato B. Nonsmooth Modeling and Simulation for Switched Circuits. Vol. 69. Springer; 2011. 33-105 p.
19. Filippov AF. Differential Equations with Discontinuous Rgihthand Sides. Kluwer Academic Publishers; 1988.
20. Hernández GG. Simulación de sistemas suaves a trozos empleando máquinas de estado finito= Simulation of piecewise smooth systems using finite state machines. bdigital.unal.edu.co [Internet]. [cited 2016 Sep 12]; Available from: http://www.bdigital.unal.edu.co/7186/
21. Urtasun A, Sanchis P, Marroyo L. Adaptive voltage control of the DC/DC boost stage in PV converters with small input capacitor. IEEE Trans Power Electron. 2013 Nov;28(11):5038–48.
22. Espinoza-Trejo DR, Bárcenas-Bárcenas E, Campos-Delgado DU, De Angelo CH. Voltage-oriented input-output linearization controller as maximum power point tracking technique for photovoltaic systems. IEEE Trans Ind Electron. 2015 Jun;62(6):3499–507.

23. Cai H, Xiang J, Wei W. Modelling , analysis and control design of a two-stage photovoltaic generation system. IET Renew Power Gener. 2016;10:1195–203.
24. Villalva MG, Gazoli JR, Filho ER. Analysis and simulationof the P&amp;#x00026;O MPPT algorithm using alinearized PV array model. 2009 Brazilian Power Electron Conf. 2009;189–95.
25. Aoun N, Chenni R, Nahman B, Bouchouicha K. Evaluation and Validation of Equivalent Five-Parameter Model Performance for Photovoltaic Panels Using Only Reference Data. Enginery Power Eng. 2014;(September):235–45.
26. Efstratios I. Batzelis IAR, Papathanassiou SA. An Explicit PV String Model Based on the Lambert Function and Simplified MPP Expressions for Operation Under Partial Shading. IEEE Trans Suntainable Energy. 2014;5.

AUTHORS

Guillermo Gallo, Electronic Engineer, MEng Industrial Automation, Ph.D. Student, Facultad de Ingeniería y Arquitectura, Universidad Nacional de Colombia Campus La Nubia, Manizales, Colombia. E-mail:ggalloh@unal.edu.co.

Juan Ruiz, Electrical and Electronic Engineer, MEng Student, Facultad de Ingeniería y Arquitectura, Universidad Nacional de Colombia Campus La Nubia, Manizales, Colombia. E-mail: jaruizt@unal.edu.co.

Mario Bolaños, Electrical and Electronic Engineer, MEng Industrial Automation, Ph.D. Student Facultad de Ingeniería y Arquitectura, Universidad Nacional de Colombia Campus La Nubia, Manizales, Colombia. E-mail: mabolanosn@unal.edu.co.

Gustavo Osorio, Electronic Engineer, MEng Industrial Automation, Ph.D. on Automation. Full Professor, Facultad de Ingeniería y Arquitectura, Universidad Nacional de Colombia Campus La Nubia, Manizales, Colombia. E-mail: gaosoriol@unal.edu.co.

Fabiola Angulo, Electrical Engineer, MEng Industrial Automation, Ph.D. on Automation. Full Professor, Facultad de Ingeniería y Arquitectura, Universidad Nacional de Colombia Campus La Nubia, Manizales, Colombia. E-mail: fangulog@unal.edu.co.